

Local structure, stripe pinning, and superconductivity in $\text{La}_{1.875}\text{Ba}_{0.125}\text{CuO}_4$ at high pressure

G. Fabbris,^{1,2} M. Hücker,³ G. D. Gu,³ J. M. Tranquada,³ and D. Haskel^{1,*}

¹*Advanced Photon Source, Argonne National Laboratory, Argonne, Illinois 60439, USA*

²*Department of Physics, Washington University, St. Louis, Missouri 63130, USA*

³*Department of Physics, Brookhaven National Laboratory, Upton, New York 11973, USA*

(Received 10 May 2013; revised manuscript received 12 August 2013; published 26 August 2013)

The interplay between stripe correlations, local structure, and superconductivity in $\text{La}_{1.875}\text{Ba}_{0.125}\text{CuO}_4$ is studied with concomitant polarized x-ray absorption fine structure (XAFS) and x-ray diffraction measurements at high pressure. Long-range order of the CuO_6 octahedral tilt pattern that pins charge-stripe order vanishes at a pressure-induced structural transition ($P = 1.8$ GPa at $T = 5$ K). Diffraction shows that static charge stripe and associated octahedral tilt correlations which survive in the high-pressure phase are effectively suppressed above 3.5 GPa. In contrast, XAFS analysis shows that instantaneous local correlations of the characteristic octahedral tilt pattern remain robust to at least 5 GPa. The decreasing local tilt angle is well correlated with a gradual increase in the superconducting transition temperature, suggesting that orientational pinning of charge correlations can survive the loss of static stripe order.

DOI: [10.1103/PhysRevB.88.060507](https://doi.org/10.1103/PhysRevB.88.060507)

PACS number(s): 74.72.-h, 61.05.cj, 74.62.Fj, 81.40.Vw

Competing electronic interactions in copper oxide, high-temperature superconductors often result in nanoscale inhomogeneity of the spin and charge density in the form of stripes, reducing the rotational symmetry of the CuO_2 planes from fourfold to twofold.¹⁻⁴ However, it is unclear whether stripe formation is purely electronically driven or triggered by distortions of the underlying crystal lattice. Two important examples are the stripe order in the La cuprate $\text{La}_{2-x}\text{Ba}_x\text{CuO}_4$, and the recently discovered charge order in the Y cuprate $\text{YBa}_2\text{Cu}_3\text{O}_{6+\delta}$.^{1,5-11} In both cases the rotational symmetry of the CuO_2 planes is either already broken or breaks at the onset of charge order. In $\text{YBa}_2\text{Cu}_3\text{O}_{6+\delta}$ the CuO chains cause an orthorhombic distortion of the CuO_2 planes.¹² In $\text{La}_{2-x}\text{Ba}_x\text{CuO}_4$ the local symmetry is reduced by a buckling of the CuO_2 planes, caused by a tilting of the CuO_6 octahedra in the low-temperature tetragonal (LTT) and low-temperature orthorhombic (LTO) phases.¹³ Understanding the energetics of competing electronic ground states and their coupling to the lattice is key towards decoding the mechanism behind high-temperature superconductivity (SC).

An effective approach to this problem is to modify the underlying crystal structure and monitor how charge order and superconductivity are affected. In a recent time-resolved ultrafast spectroscopy experiment on stripe ordered, nonsuperconducting $\text{La}_{1.675}\text{Eu}_{0.2}\text{Sr}_{0.125}\text{CuO}_4$, a compound isostructural to $\text{La}_{1.875}\text{Ba}_{0.125}\text{CuO}_4$ (LBCO_{1/8}), it was demonstrated that midinfrared pulses can induce a transient superconducting state.¹⁴ It was speculated that the light pulses distort the LTT phase and presumably destroy stripe order, but details of the coupling between charge order and crystal lattice remain unclear. Following a different approach, Ref. 15 describes how pressure suppresses the long-ranged buckling of CuO_2 planes in LBCO_{1/8}, restoring the fourfold lattice symmetry of the high-temperature tetragonal (HTT) phase. X-ray diffraction showed that charge (stripe) order (CO) still forms in the high-pressure HTT phase while SC remains suppressed. It was concluded that stripes spontaneously break the rotational symmetry of the CuO_2 planes, and are pinned by quenched buckling disorder. This suggests that the CO in LBCO_{1/8}

is strongly affected by the local structure; in fact, stripes are predicted to be pinned by local, rather than long-range, disorder.² Similarly, the short superconducting coherence length (~ 10 – 20 Å) of high T_c superconductors necessitates probing structural correlations at this length scale.

Here we study the relationship between local structure, stripe order, and SC in single crystal $\text{La}_{1.875}\text{Ba}_{0.125}\text{CuO}_4$ using simultaneous La K -edge polarized x-ray absorption fine structure (XAFS) and diffraction measurements at high pressure in a diamond anvil cell. While our diffraction data show a complete suppression of LTT long-range structural order and restoration of fourfold symmetry in the macroscopic HTT structure, XAFS data clearly indicate that the local LTT tilts persist up to the highest pressure measured (5 GPa). Neither CO nor SC show anomalies across the macroscopic LTT-HTT transition, indicating that long-range structural order does not strongly couple to electronic ordering. On the other hand, CO and LTT domains are concomitantly suppressed and the reduction in local LTT angle appears to strongly correlate with the pressure-dependent superconducting T_c , both indicative of a strong coupling of electronic ordering to local structural order.

The LBCO_{1/8} single crystal was grown with the traveling-solvent floating-zone technique. Figure 1 presents its three structural phases at ambient pressure, which can be distinguished by different patterns of tilted CuO_6 octahedra.^{6,13,15} At room temperature the average structure is HTT (space group $I4/mmm$) with untilted octahedra (lattice parameters $a = 3.78$ Å and $c = 13.2$ Å). All crystal directions and scattering vectors in this study are specified based on this unit cell. In the LTO phase ($Bmab$) below $T = 235$ K, the octahedra tilt about the $[110]$ direction, resulting in buckling distortions of all Cu-O-Cu bonds in the CuO_2 plane [see Fig. 1(b)]. At $T = 54$ K the LTT phase ($P4_2/nm$) is reached where the octahedra alternately tilt about $[100]$ and $[010]$ directions in adjacent CuO_2 planes [Fig. 1(c)]. While this restores fourfold symmetry in the macroscopic LTT structure, that of the individual planes is broken because in each plane only half of all Cu-O-Cu bonds are buckled. This anisotropy of

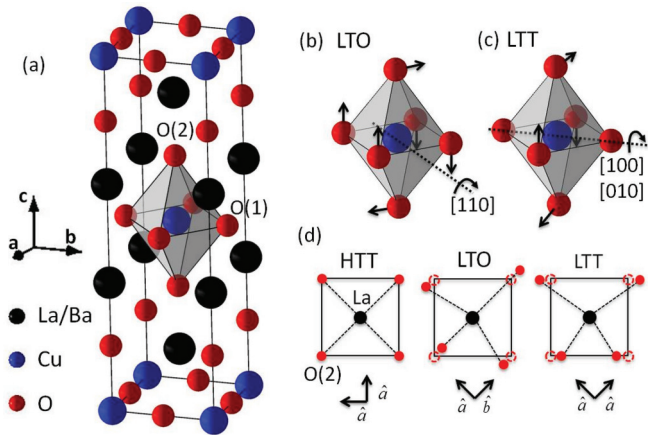


FIG. 1. (Color online) (a) HTT structure of $\text{LBCO}_{1/8}$ (Ref. 13) showing inequivalent oxygen sites. (b), (c) Rotation of CuO_6 octahedra along a Cu-Cu in-plane direction leading to the LTO structure, and along a Cu-O in-plane direction leading to the LTT structure. (d) In-plane, La-O(2) distances for HTT, LTO, and LTT phases. The LTO and LTT phases display a very different distribution of La-O(2) distances (three vs two unique bond lengths, respectively).

the LTT phase seems to be crucial for stripe pinning, as evident in the 90° rotation of stripe direction between adjacent planes.¹

The experiments were performed at undulator beamline 4-ID-D of the Advanced Photon Source, Argonne National Laboratory. X rays tuned to the La K -edge energy (38.95 keV) were used. A membrane-driven diamond anvil cell (DAC) was prepared with both full and perforated anvils, the latter mitigating the distortion of XAFS data by diamond Bragg peaks. As seen in Fig. 2(b), a small single crystal was loaded together with ruby balls and a silver foil, the latter used for *in situ* pressure calibration. The experimental setup is depicted in Fig. 2(a). Diffraction was measured in Laue (transmission) geometry. Since the crystal may slightly rotate during pressure

load, the horizontal x-ray linear polarization was aligned along the a or c axis using (006) or (200) Bragg peaks, respectively. The (100) peak, allowed in the LTT phase only, was also probed at each pressure in order to locate the LTT-HTT phase boundary. Polarized XAFS data were collected in transmission mode up to ~ 860 eV above the edge ($k \sim 15 \text{ \AA}^{-1}$), translating into $\sim 0.1 \text{ \AA}$ spatial resolution in the refinements of interatomic distances.¹⁶ XAFS spectra collected for both polarizations at 0.3 GPa are shown in Fig. 2(c). The IFEFFIT/HORAE^{17,18} and FEFF8¹⁹ packages were used to analyze the XAFS data. Additional x-ray diffraction measurements probing CO and tilt domains across the LTT-HTT phase boundary were carried out with the same setup using 20 keV x rays. See the Supplemental Material²⁰ for further details on the experimental setup and data analysis.

The large sensitivity of La K -edge polarized XAFS to the nature of local tilts in oriented samples of $\text{LBCO}_{1/8}$ was previously demonstrated at ambient pressure.¹⁶ As seen in Fig. 1(d), the rotations of CuO_6 octahedra in LTT and LTO phases introduce strong splittings in the in-plane La-O(2) distances ($\sim 0.15\text{--}0.2 \text{ \AA}$), whereas a single planar La-O(2) distance is present in the HTT phase. XAFS measurements on powder samples, on the other hand, average over all nine La-O distances, reducing the sensitivity to the different tilt patterns. There are few reports on the use of polarized XAFS at high pressures,^{21–23} and to our knowledge simultaneous measurements of single crystal diffraction and polarized XAFS to high photoelectron wave number, $k = 15 \text{ \AA}^{-1}$, under high pressure in a diamond anvil cell still need to be reported.

At ambient pressure the XAFS data is best fitted with an LTT model as expected from diffraction¹³ and previous XAFS studies¹⁶ [Figs. 3(a) and 3(c)]. Figures 3(b) and 3(d) show fits to the 2.7 GPa data for both polarizations using LTT and HTT models. At this pressure the system is in the macroscopic HTT phase [Fig. 4(c)]. While the $\hat{e} \parallel c$ data has low sensitivity to local tilts [Fig. 3(b)], the $\hat{e} \parallel a$ XAFS data is highly sensitive to local tilts and can only be described with an LTT model [Fig. 3(d)]. In fact, the R factor (misfit) for the first coordination shell in the LTT model is 4.3%, while for the HTT model it is 13.6%. Furthermore, the back Fourier transform (FT) of first shell La-O distances in the $\hat{e} \parallel a$ data is in very good agreement with an LTT model [Fig. 3(e)], while the HTT model completely misses the beating pattern arising from splittings in La-O distances as a result of local LTT tilts. Finally, the pressure dependence of the measured root-mean-squared (rms) disorder in the La-O bond length further supports the persistence of local LTT tilts at high pressures. An HTT model results in an unphysical increase in rms disorder across the LTT-HTT phase transition [Fig. 3(f)]. Fits with a pure LTO model could not reproduce the data and models combining LTT/HTT and LTT/LTO mixtures resulted in over 95% LTT phase fraction. Further details on XAFS modeling are presented in the Supplemental Material.²⁰

While these results clearly show that local LTT tilts persist well into the macroscopic HTT phase (at least to 5 GPa), we observe a clear reduction in the La-O(2) splitting with pressure [Figs. 4(a) and 4(b)], indicative of a reduction in the local tilt angle of rigid CuO_6 octahedral units. A concomitant reduction in La-O(1) and La-La distance splittings is also observed, consistent with this picture. As previously reported,^{24,25} the larger

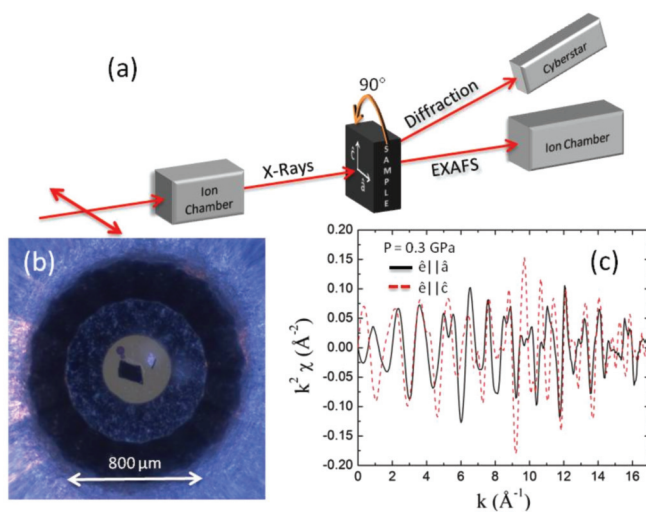


FIG. 2. (Color online) (a) Experimental setup. The sample surface contains both a and c axes. (b) Diamond anvil cell showing the sample (near center), Ag foil used for *in situ* pressure calibration, and two ruby balls used for pressure calibration during sample loading. (c) XAFS, $\chi(k)$, data for the two polarizations at $P = 0.3 \text{ GPa}$ and $T = 5 \text{ K}$.

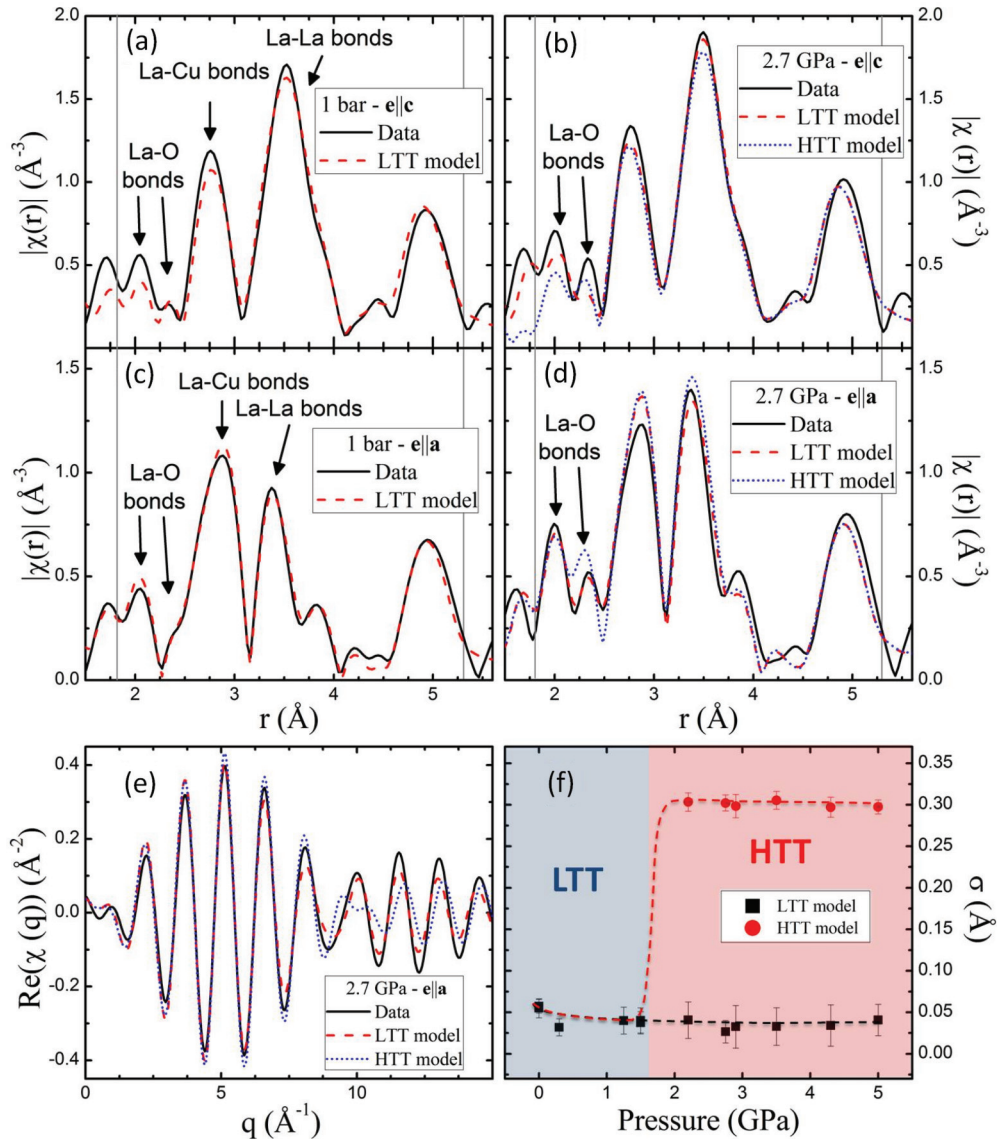


FIG. 3. (Color online) (a), (c) Magnitude of FT-XAFS data for both polarizations taken at ambient pressure ($T = 5$ K) together with a fit to an LTT model. (b), (d) Magnitude of FT-XAFS data for both polarizations taken at $P = 2.7$ GPa, $T = 5$ K (well within the macroscopic HTT phase). (e) Back FT of $\hat{e} \parallel a$ XAFS data in the $r = (1.7-2.5)$ Å region containing the La-O distances. (f) Fitted rms disorder in La-O bond length using LTT and HTT models.

compressibility of the rocksalt LaO_2 layer relative to that of the CuO_2 layer is the likely cause for the tilt reduction under pressure. The single La-O(2) planar distance in the macroscopic HTT phase, as obtained from lattice parameters measured in the simultaneous diffraction experiment, is in good agreement with an average of the two local La-O(2) distances obtained by XAFS within the LTT model [Fig. 4(a)], indicating that the macroscopic HTT phase is recovered by long-range averaging of local distortions. We note that the La-O(2) splitting evolves smoothly across the LTT-HTT transition, with no evidence of any discontinuity. The survival of instantaneous local LTT tilt correlations across a structural transition is not without precedent, as it has been observed previously across thermally induced transitions (at ambient pressure) in both $\text{LBCO}_{1/8}$ (Refs. 16 and 26) and $\text{La}_{1.8-x}\text{Eu}_{0.2}\text{Sr}_x\text{CuO}_4$ (Ref. 27) and tilt correlations also survive the doping-induced loss of tilt order in $\text{La}_{2-x}\text{Sr}_x\text{CuO}_4$.²⁸

The presence of local LTT tilts in the high-pressure HTT phase is demonstrated, but XAFS is unable to provide information on how (and if) such tilts order at intermediate length scales and interact with short-ranged CO. To study this relationship, guided by previous findings,¹⁵ we probed the high-pressure behavior of both $(1.5, 1.5, 2)$ LTT/LTO and $(2 - 2\delta, 0, 0.5)$ CO diffraction peaks. The width of the structural superlattice peak undergoes a drastic change from sharp to broad across the LTT-HTT transition at $p_c \sim 1.8$ GPa [Fig. 5(a)], consistent with the persistence of LTT domains, ~ 80 Å in size, in the HTT phase. CO domains appear to be strongly correlated with these LTT domains as both display the same correlation length [Fig. 5(b)] and collapse together at higher pressures [Fig. 5(c)] to become undetectable by x-ray diffraction above 3.5 GPa. These results suggest that CO needs local LTT order in $\text{LBCO}_{1/8}$ and that they spatially coexist. However, the origin of stripe pinning in the macroscopic HTT

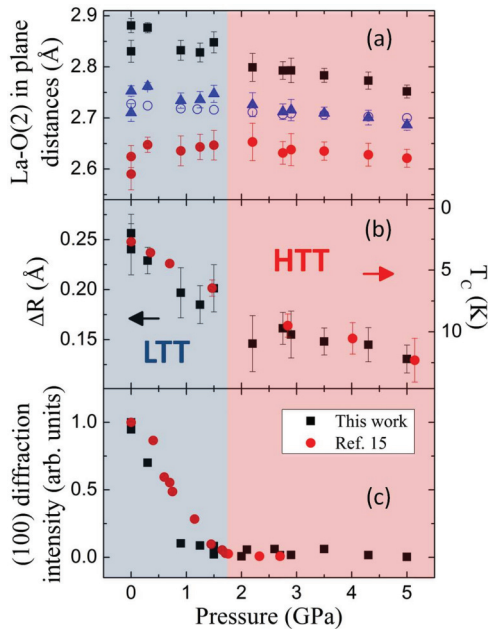


FIG. 4. (Color online) (a) Pressure dependence of in-plane La-O(2) distances (black squares and red circles). The average of these local distances (solid blue triangles) is in good agreement with the average distance measured by diffraction (open blue circles). (b) Pressure dependence of the La-O(2) splitting (black squares) and T_c (red circles) (Ref. 15). (c) Pressure dependence of LTT-(100) peak intensity together with results from Ref. 15. Both data were normalized to unity at ambient pressure for clarity.

phase remains unclear with either the LTT domains driving stripe pinning, or stripe order driving the formation of local LTT domains.

It is known that the strongly depressed bulk T_c in $\text{LBCO}_{1/8}$ is caused by frustration of the interlayer Josephson coupling, which occurs as a consequence of the charge-stripe order and the interlayer rotation of the stripe-pinning anisotropy associated with the LTT phase.^{29,30} We have shown that elastic scattering from charge-stripe order is continuously depressed at high pressure in the HTT phase ($p > p_c$), and becomes negligible above ~ 3.5 GPa. One might expect to see a rapid rise in T_c associated with the disappearance of the static stripe order; however, even at 5 GPa (15 GPa), T_c has only reached 12 K (18 K),¹⁵ which is far below the 40 K onset of strong superconducting correlations within the CuO_2 layers at ambient pressure,³¹ as well as the highest observed bulk T_c of 32 K.⁷ Instead, we observe that $\Delta T_c(P) \sim -\Delta R(P)$, where ΔR is the La-O(2) splitting [Fig. 4(b)].³² Although the current experiments only probe the instantaneous lattice/electronic ordering and average over their dynamics, given the close

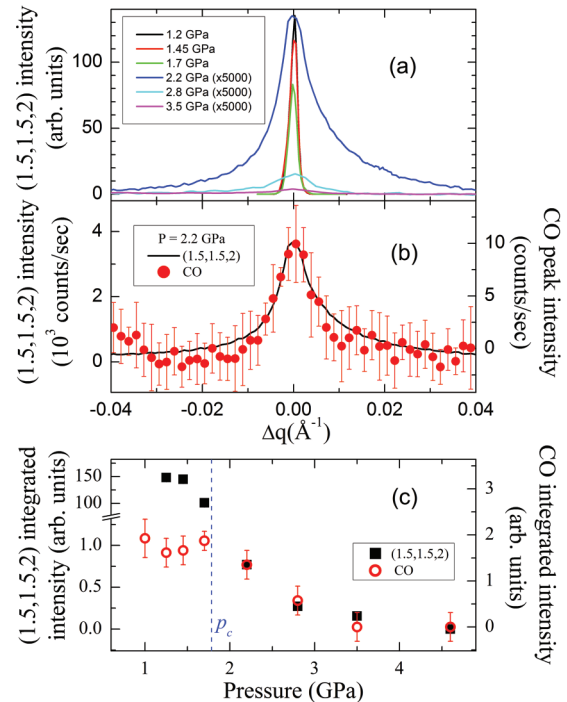


FIG. 5. (Color online) (a) Pressure dependence of (1.5,1.5,2) (h,k) scans at $T = 5$ K. A significant drop in intensity is observed across the LTT-HTT transition at $p_c \sim 1.8$ GPa, but diffuse scattering from ~ 80 Å distorted domains remains present in the HTT phase. (b) Above 1.7 GPa the (1.5,1.5,2) peak has the same width as that of the $(2 - 2\delta, 0, 0.5)$ CO peak (h scan), indicating the coexistence of CO and distorted structural domains. (c) Integrated intensity of (1.5,1.5,2) (hk scan) and $(2 - 2\delta, 0, 0.5)$ (h scan) peaks as a function of pressure.

connection between the LTT tilt pattern and stripe order, we infer from the T_c correlation that the local LTT tilt correlations are sufficient to pin a charge nematic state,² involving slowly fluctuating charge stripes, that retains the partially frustrated Josephson coupling. This is evidence, if somewhat indirect, for a dynamical phase with intertwined charge and superconducting order.³⁰ A challenging experiment for the future would be to investigate the evolution of low-energy spin fluctuations with pressure in order to follow their relationship with the superconductivity.

Work at Argonne National Laboratory (Brookhaven National Laboratory) is supported by the US Department of Energy, Office of Science, Office of Basic Energy Sciences, under Contract No. DE-AC02-06CH11357 (DE-AC02-98CH10886). We would like to thank Yejun Feng for his valuable advice and help during the experiment.

*haskel@aps.anl.gov

¹J. M. Tranquada, B. J. Sternlieb, J. D. Axe, Y. Nakamura, and S. Uchida, *Nature (London)* **375**, 561 (1995).

²S. A. Kivelson, E. Fradkin, and V. J. Emery, *Nature (London)* **393**, 550 (1998).

³Y. Kohsaka, C. Taylor, K. Fujita, A. Schmidt, C. Lupien, T. Hanaguri, M. Azuma, M. Takano, H. Eisaki,

H. Takagi, S. Uchida, and J. C. Davis, *Science* **315**, 1380 (2007).

⁴D. Haug, V. Hinkov, Y. Sidis, P. Bourges, N. B. Christensen, A. Ivanov, T. Keller, C. T. Lin, and B. Keimer, *New J. Phys.* **12**, 105006 (2010).

⁵M. Fujita, H. Goka, K. Yamada, J. M. Tranquada, and L. P. Regnault, *Phys. Rev. B* **70**, 104517 (2004).

- ⁶Y.-J. Kim, G. D. Gu, T. Gog, and D. Casa, *Phys. Rev. B* **77**, 064520 (2008).
- ⁷M. Hücker, M. v. Zimmermann, G. Gu, Z. Xu, J. Wen, G. Xu, H. Kang, A. Zheludev, and J. Tranquada, *Phys. Rev. B* **83**, 104506 (2011).
- ⁸G. Ghiringhelli, M. L. Tacon, M. Minola, S. Blanco-Canosa, C. Mazzoli, N. B. Brookes, G. M. D. Luca, A. Frano, D. G. Hawthorn, F. He, T. Loew, M. M. Sala, D. C. Peets, M. Salluzzo, E. Schierle, R. Sutarto, G. A. Sawatzky, E. Weschke, B. Keimer, and L. Braicovich, *Science* **337**, 821 (2012).
- ⁹J. Chang, E. Blackburn, A. T. Holmes, J. Larsen, J. Mesot, R. Liang, S. A. Bonn, W. N. Hardy, A. Watenphul, M. v. Zimmermann, E. M. Forgan, and S. M. Hayden, *Nat. Phys.* **8**, 871 (2012).
- ¹⁰E. Blackburn, J. Chang, M. Hücker, A. T. Holmes, N. B. Christensen, R. Liang, D. A. Bonn, W. N. Hardy, U. Rütt, O. Gutowski, M. v. Zimmermann, E. M. Forgan, and S. M. Hayden, *Phys. Rev. Lett.* **110**, 137004 (2013).
- ¹¹S. Blanco-Canosa, A. Frano, T. Loew, Y. Lu, J. Porras, G. Ghiringhelli, M. Minola, C. Mazzoli, L. Braicovich, E. Schierle, E. Weschke, M. Le Tacon, and B. Keimer, *Phys. Rev. Lett.* **110**, 187001 (2013).
- ¹²M. v. Zimmermann, J. R. Schneider, T. Frello, N. H. Andersen, J. Madsen, M. Käll, H. F. Poulsen, R. Liang, P. Dosanjh, and W. N. Hardy, *Phys. Rev. B* **68**, 104515 (2003).
- ¹³J. D. Axe, A. H. Moudden, D. Hohlwein, D. E. Cox, K. M. Mohanty, A. R. Moodenbaugh, and Y. Xu, *Phys. Rev. Lett.* **62**, 2751 (1989).
- ¹⁴D. Fausti, R. I. Tobey, N. Dean, S. Kaiser, A. Dienst, M. C. Hoffmann, S. Pyon, T. Takayama, H. Takagi, and A. Cavalleri, *Science* **331**, 189 (2011).
- ¹⁵M. Hücker, M. v. Zimmermann, M. Debessai, J. S. Schilling, J. M. Tranquada, and G. D. Gu, *Phys. Rev. Lett.* **104**, 057004 (2010).
- ¹⁶D. Haskel, E. A. Stern, F. Dogan, and A. R. Moodenbaugh, *Phys. Rev. B* **61**, 7055 (2000).
- ¹⁷M. Newville, *J. Synchrotron Radiat.* **8**, 322 (2001).
- ¹⁸B. Ravel and M. Newville, *J. Synchrotron Radiat.* **12**, 537 (2005).
- ¹⁹A. L. Ankudinov, B. Ravel, J. J. Rehr, and S. D. Conradson, *Phys. Rev. B* **58**, 7565 (1998).
- ²⁰See Supplemental Material at <http://link.aps.org/supplemental/10.1103/PhysRevB.88.060507> for details on the experimental setup and XAFS data analysis.
- ²¹J. Pellicer-Porres, A. Segura, V. Munoz, and A. San Miguel, *Phys. Rev. B* **61**, 125 (2000).
- ²²A. San-Miguel, J. Pellicer-Porres, A. Segura, J. P. Itié, A. Polian, and M. Gauthier, *High Pressure Res.* **19**, 335 (2000).
- ²³J. Pellicer-Porres, A. Segura, C. Ferrer, V. Muñoz, A. S. Miguel, A. Polian, J. P. Itié, M. Gauthier, and S. Pascarelli, *Phys. Rev. B* **65**, 174103 (2002).
- ²⁴H. Takahashi, H. Shaked, B. A. Hunter, P. G. Radaelli, R. L. Hitterman, D. G. Hinks, and J. D. Jorgensen, *Phys. Rev. B* **50**, 3221 (1994).
- ²⁵M. K. Crawford, R. L. Harlow, S. Deemyad, V. Tissen, J. S. Schilling, E. M. McCarron, S. W. Tozer, D. E. Cox, N. Ichikawa, S. Uchida, and Q. Huang, *Phys. Rev. B* **71**, 104513 (2005).
- ²⁶S. J. L. Billinge, G. H. Kwei, and H. Takagi, *Phys. Rev. Lett.* **72**, 2282 (1994).
- ²⁷S.-H. Baek, P. C. Hammel, M. Hücker, B. Büchner, U. Ammerahl, A. Revcolevschi, and B. J. Suh, *Phys. Rev. B* **87**, 174505 (2013).
- ²⁸E. S. Bozin, S. J. L. Billinge, G. H. Kwei, and H. Takagi, *Phys. Rev. B* **59**, 4445 (1999).
- ²⁹A. Himeda, T. Kato, and M. Ogata, *Phys. Rev. Lett.* **88**, 117001 (2002).
- ³⁰E. Berg, E. Fradkin, S. A. Kivelson, and J. M. Tranquada, *New J. Phys.* **11**, 115004 (2009).
- ³¹Q. Li, M. Hücker, G. D. Gu, A. M. Tsvelik, and J. M. Tranquada, *Phys. Rev. Lett.* **99**, 067001 (2007).
- ³²Extrapolation of ΔR to zero yields $T_c \sim 25$ K, lower than optimal T_c values, so additional sources of T_c suppression cannot be ruled out.